Analytical Chemistry **2010,** *82,* 3531–3536

doi: 10.1021/ac902554v

Label-free sub-picomolar protein detection with field-effect transistors

Pedro Estrela [*,a,1], *Debjani Paul* [1], *Qifeng Song* [2], *Lukas K. J. Stadler* [2], *Ling Wang* [3], *Ejaz Huq* [3], *Jason J. Davis* [4], *Paul Ko Ferrigno* [2], *Piero Migliorato* [1]

[1] University of Cambridge, Department of Engineering, Electrical Engineering Division, 9 J.J. Thomson Avenue, Cambridge CB3 0FA, UK

[2] Leeds Institute of Molecular Medicine, St. James's University Hospital, Leeds LS9 7TF, UK

[3] Rutherford Appleton Laboratory, Central Microstructure Facility, Chilton, Didcot OX11 0QX, UK

[4] University of Oxford, Department of Chemistry, Physical and Theoretical Chemistry Laboratory, South Parks Road, Oxford OX1 3QZ, UK

[*] Corresponding author. Fax: +44-1225-386305, p.estrela@bath.ac.uk

[a] Current address: University of Bath, Department of Electronic & Electrical Engineering, Bath BA2 7AY, UK

ABSTRACT

Proteins mediate the bulk of biological activity and are powerfully assayed in the diagnosis of diseases. Protein detection relies largely on antibodies, which have significant technical limitations especially when immobilised on two-dimensional surfaces. Here, we report the integration of peptide aptamers with extended gate metal-oxide-semiconductor field-effect transistors (MOSFETs) to achieve label free sub-picomolar target protein detection. Specifically, peptide aptamers that recognise highly related protein partners of the cyclin-dependent kinase (CDK) family are immobilized on the transistor gate to enable human CDK2 to be detected at 100 fM or 5 pg/ml, well within the clinically relevant range. The target specificity, ease of fabrication and scalability of these FET arrays, further demonstrates the potential application of the multiplexable field effect format to protein sensing.

KEYWORDS

Label-free detection, field effect transistors, protein interactions, peptide aptamers.

A detailed understanding of complex biological systems requires information about the functional state of proteins, which perform the bulk of the work on the cell. The introduction of monoclonal antibodies[1] allowed the development of a number of robust detection techniques that are largely suitable for the detection of protein expression, one protein species at a time.[2] The sequencing of the human genome has revealed that protein complexity is much more subtle than previously suspected, with multiple protein isoforms being encoded by relatively few genes: the genome of *Homo sapiens* comprises just 6,000 more genes than, for example, that of the nematode worm *Caenorhabditis elegans* (25,000 compared to 19,000). Thus, genome sequencing and DNA microarrays have revealed that several variant messenger RNAs are made from each gene. Moreover, multiple protein isoforms carrying differential chemical modifications are made from each mRNA variant. New technologies that will allow the highly multiplexed detection of many highly related protein isoforms simultaneously are therefore now urgently sought.[3] Our inability to detect, measure and monitor this complexity leads to a large gap in our ability to understand biology and devise new treatments for disease. Proteomics is currently playing a major role in cataloguing proteins, to great effect in many areas such as the identification of cancer biomarkers.[4] However, the state-of-the-art technologies suffer from many limitations. For example, mass spectrometry is able to produce signatures indicating a pattern of protein expression, but cannot routinely simultaneously identify the proteins that constitute that pattern. In addition, whilst a catalogue of proteins expressed in a given situation is the first step to understanding the underlying biology, it is also necessary to be able to determine the activation state of each protein. This is because the ability of each protein to interact with its substrates or partners is regulated by post-translational, chemical modifications that alter or stabilise specific conformations or shapes in each protein to drive or prevent interactions with specific partners. To take such a detection ability to a high-throughput quantitative format is highly desirable, particularly if the low detection limits required clinically can, additionally, be realised.

Several studies on the use of technologies developed for DNA microarrays for the characterization of proteomes are presently underway.[5,6] Although these approaches had some success in protein expression profiling, the scope of applications has been limited. One of the main aspects hampering the development of these array-based approaches is the need to use labels such as enzymes or fluorescent tags. Unlike the case of DNA, labelling a protein with a molecular tag can strongly affect its binding properties and the yield of the target-label coupling reaction is highly variable.[7]

Label-free electrical detection techniques suitable for protein interactions are therefore of considerable interest. Several electrochemical techniques have been proposed for the detection of proteins.[8-10] Impedance-based sensors and field-effect devices, in particular, are promising candidates for the development of inexpensive microarrays associated with portable instrumentation. Field-effect transistors with metal gate electrodes, such as those previously developed for DNA sensing,[11] are an example of such sensors. These stable semiconductor devices measure variations in the open circuit potential (OCP) that occur at the metal gate interface when the charge density and distribution of the immobilized bio-layer change upon interaction with a target biomolecule.

A major limitation in the production of devices for the detection of biomolecules, however, is the availability of robust probes that are able to specifically detect the target biomolecule. Traditionally, antibodies have been the affinity probes of choice in biology. Antibodies are proteins that comprise a constant region that interacts with effectors of the immune system and the variable recognition moiety, which specifically recognizes and binds to target molecules. However, many antibodies are found to lose their specificity when immobilized on surfaces.[12] A range of alternative affinity probes exist, including engineered proteins that do not use the antibody scaffold.[13] In common with these, peptide aptamers are artificial proteins

engineered to possess the affinity and specificity of antibodies, but they differ from the other engineered proteins in being designed to retain their integrity within the context of a eukaryotic cell.[14] The peptide aptamer scaffold is thus chosen for its biological simplicity and structural stability. As with the variable region of antibodies, peptides inserted into the primary sequence of the scaffold (by manipulation of the gene encoding it) are forced to adopt a particular fold dictated by the folding of the scaffold, and become able to bind to specific partners with high specificity and affinity.[13,14] We have introduced a new non-antibody scaffold, called Stefin A Triple Mutant (STM) that lacks significant affinity for human proteins[15] and have been able to show that peptide aptamers presented by STM can be immobilized using a range of surface chemistries while still retaining the ability to detect their partners.[16-21] Of key relevance here, protein detection has recently been achieved by direct differential measurement of OCP variations using an ultra-low input bias current instrumentation amplifier.[17] The biological system assessed here consisted of a panel of peptide aptamers that recognise specific protein partners of the cyclin-dependent kinase (CDK) family, whose activity is important in proliferating and cancerous cells.

We report here the use of extended gate metal-oxide-semiconductor field-effect transistors (MOSFETs) for label-free electrical detection of proteins. Low-leakage single-crystalline MOSFETs fabricated using Complementary Metal–Oxide–Semiconductor (CMOS) technology were connected to external gold electrodes on which orientated peptide aptamers were covalently immobilized. The interaction between the peptide aptamers and the protein CDK2 (a protein known to be active in proliferating cells, including cancer cells) was probed as a test study for a generic sensitive method for detection of protein interactions. Concentration profiles were obtained showing an ultra-low protein detection limit.

EXPERIMENTAL SECTION

Protein preparation. Details of peptide aptamers, protein expression and purification, have been reported elsewhere.[15,16,18] The expression vector used drives the incorporation of a single cysteine residue in the amino-terminal tail encoded by the pHTLV1 vector in order to allow a controllable immobilization on gold substrates. STM^{Cys+} and STM^{Cys+}–pep2 were expressed as hexahistidine fusion proteins in Escherichia coli cells. The full amino acid sequences of STM, STM^{Cys+} and STM^{Cys+}–pep2 are presented in Table 1. Including the Cys+ extension, STM is 159 amino acids long and has a predicted molecular weight of 18 kDa while STM-pep2 is 181 amino acids long with a predicted molecular weight of 20 kDa. Recombinant CDK2 was purchased from Abnova (Taiwan). A CDK-free yeast lysate was used as a control.[17-18] Briefly, the CDK2 gene was cloned into the yeast expression vector pDEST32 (Invitrogen) and transformed into MAV203 yeast cells as described previously.[17-18]. A 5 ml culture of yeast was grown in selective dropout medium lacking leucine to OD_{600}=4 (corresponding to $0.8x10^8$ cells/mL). The culture was then centrifuged for 10 min at 3200 × *g*, the supernatant removed and the cell pellet resuspended in 400 μl of Y-Per™ yeast protein extraction reagent (Pierce) with protease inhibitor (Roche). The protein extraction reaction was performed at room temperature with regular vortexing for 30 min. The sample was then submitted to centrifugation at 16,000 × *g* for 10 min and the soluble fraction stored at -80°C until use. Human cell lysate was prepared from actively proliferating human DG75 cells that express CDK2. DG75 cells were grown in RPMI medium (GIBCO) supplemented with 10% fetal bovine serum, 50 U/mL penicillin and 50 μg/mL streptomycin. The cells were collected, washed with pre-chilled PBS (pH 7.2) and lysed by sonication in lysis buffer (20 mM HEPES, pH 7.5, 150 mM KCl, 0.1 mM EDTA, 10% glycerol, 0.1% NP-40, 1 mM DTT, protease inhibitor cocktail (Roche), 1 mM PMSF) at 4°C. The resulting cell lysate was centrifuged with an Eppendorf 5310R at 13,000 rpm for 20 minutes at 4°C. The supernatant was transferred to pre-chilled clean vials, flash-frozen and stored at -80°C until use.

Table 1. Amino acid sequence and size of STM, STM^{Cys+} and STM^{Cys+}-pep2.

protein	*sequence*	*number of amino acids*	*estimated molecular weight (Da)*
STM	mipwglseakpatpeiqeivdkvkpqleektnetygkleavqyktqvdagtnyyikvragdnkymhlkvfngppgqnedlvltgyq vdknkddeltgf	98	11074
STM^{Cys+}	MHHHHHHSSGLVPCGSGMKETAAAKFERQHMDSPDLGTWSHPQFEKYDDDDKAMADIGSE Fmipwglseakpatpeiqeivdkvkpqleektnetygkleavqyktqvdagtnyyikvragdnkymhlkvfngppgqnedlvltgy qvdknkddeltgf	159	17950
STM^{Cys+}-pep2	MHHHHHHSSGLVPCGSGMKETAAAKFERQHMDSPDLGTWSHPQFEKYDDDDKAMADIGSE Fmipwglseakpatpeiqeivdkvkpqleektnetygkleavqyktqvdagtnyyikvragdnkymhlkvfngp**LVCKSYRL DWEAGALFRSLF**gppgqnedlvltgyqvdknkddeltgf	181	20461

Notes: The Cys+ tail is presented in capital letters and the pep2 insert in bold capital letters. The cysteine in position 14 (underlined) is used for the immobilization of the proteins.

Materials. All chemicals were purchased from Sigma-Aldrich (UK) with the exception of the thiolated polyethylene glycol (Asemblon, USA). All proteins and lysates were diluted to the desired concentration in 10 mM phosphate buffer (PB) pH 7.2. Buffers were prepared by mixing the appropriate amounts of KH_2PO4 and K_2HPO4 using ultra pure deionized water (18.2 MΩ.cm resistivity). The total ionic strength of the phosphate buffer amounts to 21 mM. The concentrations presented for the lysates refer to the total concentration of all cellular proteins in the lysate.

Field-effect transistor set-up. Single-crystalline Si MOSFETs were fabricated using a CMOS 0.7 µm process at IMEC (Belgium). The devices have no electrostatic discharge (ESD) protection elements in order to minimize their gate leakage current. Each chip contains five n-type MOSFETs with a common source contact. Different sized transistors have been used with widths (W) and lengths (L) ranging from 1340 µm to 3860 µm and 2.0 µm to 0.7 µm, respectively, while keeping the W×L product at approximately 2700 μm^2. The chip was glued on a glass substrate containing evaporated gold electrodes (100 nm Au with 10 nm Cr as adhesion layer) consisting of a bonding pad connected to a 500 µm x 500 µm pad. The on-chip gate contact pads were wire-bonded to the Au electrodes as shown in figure 1 and the source, drain and substrate contact pads were wire-bonded to a printed circuit board (PCB). The chip was first passivated with Glob-Top (Amicon) epoxy encapsulant and then both the chip and the Au bonding wires were passivated with a low viscosity silicone rubber (3140 RTV coating from Dow Corning). The Au electrodes on the glass substrate were patterned with 50 µm SU-8 to open 380 µm x 380 µm windows on top of the Au pad. When the glass chip is immersed in an electrolyte, only these exposed Au areas are in contact with the solution. The characteristics of the transistors were measured using a semiconductor parameter analyzer (HP4156A, Hewlett Packard, USA). It should be noted that instabilities were observed on a few chips resulting in abnormally high shifts in transfer characteristics upon interaction with a target (specific or otherwise). On these chips a strong time dependence of the signals was observed and all the transistors in the same chip showed very different signals – these criteria were used to identify unstable chips.

Immobilization and interaction procedures. Prior to protein immobilization, the Au electrodes were rinsed with acetone and then isopropanol. The electrodes were then cleaned in a UV/Ozone system (Novascan PSD-UVT, USA) followed by ethanol and ultra-pure water rinses. Cysteine modified STM or STM-pep2 was immobilized from a 1 µM solution in 10 mM phosphate buffer (PB)

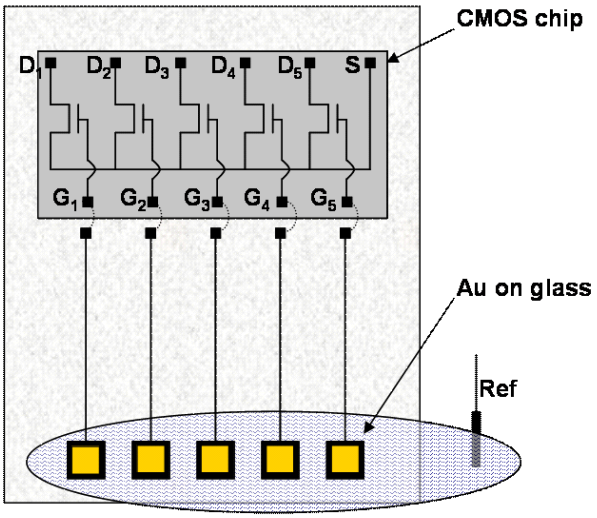

Figure 1. Schematic structure of a linear array of five MOSFETs with extended gold gates. The gate contact pads are wire-bonded to gold electrodes evaporated on glass. Only the gold pad electrodes are exposed to the electrolyte. S, $D_{1\text{-}5}$ and $G_{1\text{-}5}$ are the on-chip contact pads for source, drains and gates, respectively.

pH 7.2 onto the freshly cleaned gold electrodes for 1.5 hours in a humidity chamber. Prior work has demonstrated the retention of robust and specific biorecognition on both bare and modified gold electrode surfaces.[16-18] The thickness of an STM^{Cys+} layer has previously been measured to be 2.7 nm by dual polarization interferometry.[18] After rinsing in the same buffer to remove unbound peptide aptamers, the exposed gold areas were passivated with a thiolated alkane polyethylene glycol (PEG) by exposing the electrodes to a 50 µM solution of $HS(CH_2)_{11}(OCH_2CH_2)_3OH$ in 10 mM PB for 1.5 h in a humidity chamber. The samples were subsequently rinsed in buffer to remove any non-immobilized molecules.

Throughout the measurements the substrate was kept grounded through the source while in between measurements the electrolyte was kept connected to the source. The transistor's transfer characteristics were measured with the drain to source voltage, V_{DS}, held at 1 V. The gate to source voltage, V_{GS}, was applied through a Hg/Hg_2SO_4 reference electrode immersed in the measurement electrolyte via a salt bridge. V_{GS} was varied between -0.5 V and +2 V and the drain current was measured. Only the transistors that showed no hysteresis were used in the present study.

The functionalized electrodes were exposed to lysates containing the target protein CDK2 as well as high concentrations of non-specific proteins for 30 minutes in a humidity chamber, followed by rinsing in buffer. The transfer characteristics of the transistors were measured before and after incubation. Parallel shifts of the transfer characteristics are observed upon interaction. The voltage shifts here presented were taken at $I_D = 1$ µA.

Transistor response concentration profiles were measured by injecting 10-20 µl of pre-concentrated stock solutions of recombinant CDK2 into a measurement cell containing 1.5 ml of 10 mM PB pH 7.2. Upon injection, the solution was stirred for 15 min with a magnetic stirrer to allow uniform mixing of the protein with the buffer and then allowed to thermally equilibrate for 15 min at room temperature. The measurements were carried out with the magnetic stirrer switched off to reduce noise.

RESULTS AND DISCUSSION

When a bio-layer is immobilized on an electrode bathed in a solution of electrolyte, the change in the charge density and/or distribution at the interface between the electrode and the electrolyte brought about by a biomolecular interaction induces a change in the open circuit potential (OCP) of the system. Although reliable measurements of OCP variations in protein systems have been achieved recently using an ultra-low input bias current instrumentation amplifier,[17] better sensitivities in OCP measurements can be achieved with field-effect transistors (FETs) since parasitic capacitances are minimized. FETs have inherent amplification, high-input impedance, low-output impedance, and potential for miniaturization and multiplexing. When the bio-layer is immobilized at the FET's metal gate, variations in the OCP brought about by a biomolecular interaction are accurately measured by a shift in the transfer characteristics (drain current I_D versus gate voltage V_{GS}) of the

FET, as previously demonstrated for the detection of DNA hybridization.[11]

In order to take advantage of previously developed STM^{Cys+} immobilization protocols,[16] gold electrodes were externally connected to the aluminium gate contact pads of the MOSFETs. Special care has to be taken during the electrode connection to avoid device failure due to electrostatic discharge (ESD) effects. As the gate voltage is applied on these external gold electrodes, any change in the OCP modulates the transistor's gate voltage. This approach creates in effect an extended-gate structure. This configuration has the advantage that the FET itself is not exposed to the electrolyte. This prevents the typical effects of signal drift caused by permeability of the gate dielectric to alkaline cations.[22]

As the gate voltage with respect to the source is applied on the reference electrode immersed in the bulk of the electrolyte, the transfer characteristics are expected to shift positively upon an increase of negative charge or a decrease of positive charge at the bio-layer interface. Negative shifts are expected upon the reverse charge variations. The device is then sensitive to variations in charge distribution at the gold electrode. Previous work has demonstrated that variations in the charge distribution at the bio-layer induces changes in the OCP, which can be measured by the use of suitable instrumentation.[17] In order to confirm that the same variations in OCP can also be measured with our FET set-up, the scaffold protein without a peptide insert, STM^{Cys+}, was immobilized on the gold electrodes and the transfer characteristics of the transistor measured at different pH values of a 10 mM phosphate buffer. We find that the MOSFET response is pH-independent when no biomolecule is immobilized on the gold electrode (data not shown). However, changes in the surface charge of immobilized STM^{Cys+} occur upon variations in the pH of the electrolyte, due to protonation/deprotonation of solvent-exposed amino acid side-chains. Since the aptamer layer thickness[18] is comparable to the Debye length of the measurement buffer (~2.5 nm) these protein charge variations are directly detectable at the

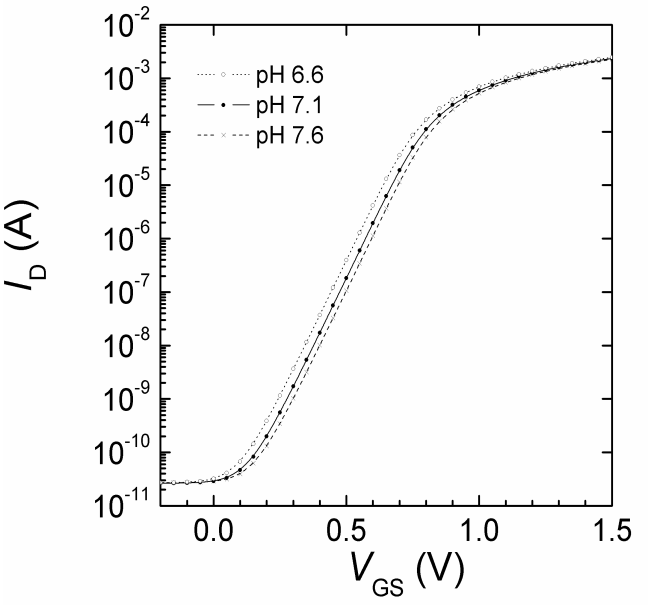

Figure 2. Transfer characteristics of a STM^{Cys+} functionalized n-channel transistor with size W/L = 3860 µm/0.7 µm upon variations of pH of the measurement electrolyte. The pH of the 10 mM PB buffers was varied between pH 6.6 and pH 7.6. V_{DS} was kept at 1 V. The error bars are smaller than the data points and were removed from the figure.

electrode. In the example shown in figure 2, the transfer characteristics shift by +32.7 mV on changing pH from 6.6 to 7.1 and by +23.2 mV on changing pH from 7.1 to 7.6. The measurements were carried out in the pH sequence of 7.1 → 7.6 → 6.6. On returning the buffer to pH 7.1, the curve returned to its original position within 0.3 mV. Similar voltage shifts were confirmed with different devices. Variations in the total ionic strength of the PB solutions associated with the pH changes have been shown to account for only a small amount of the total OCP variation.[17] These results demonstrate that our devices are sensitive to variations in protein charge brought about by varying the pH of the surrounding electrolyte.

The use of CMOS MOSFETs with externally connected gold electrodes for the detection of protein interactions was studied for the peptide aptamer STM^{Cys+}–pep2, which has a strong interaction with the protein CDK2.[15,19] Figure 3 shows the transfer characteristics of two MOSFETs after immobilization of the peptide aptamer. Upon interaction with a human cell lysate expressing CDK2, a shift of +26.7 ± 3.8 mV is observed (figure 3a). The direction of the shift is consistent with the results obtained with direct OCP measurements for

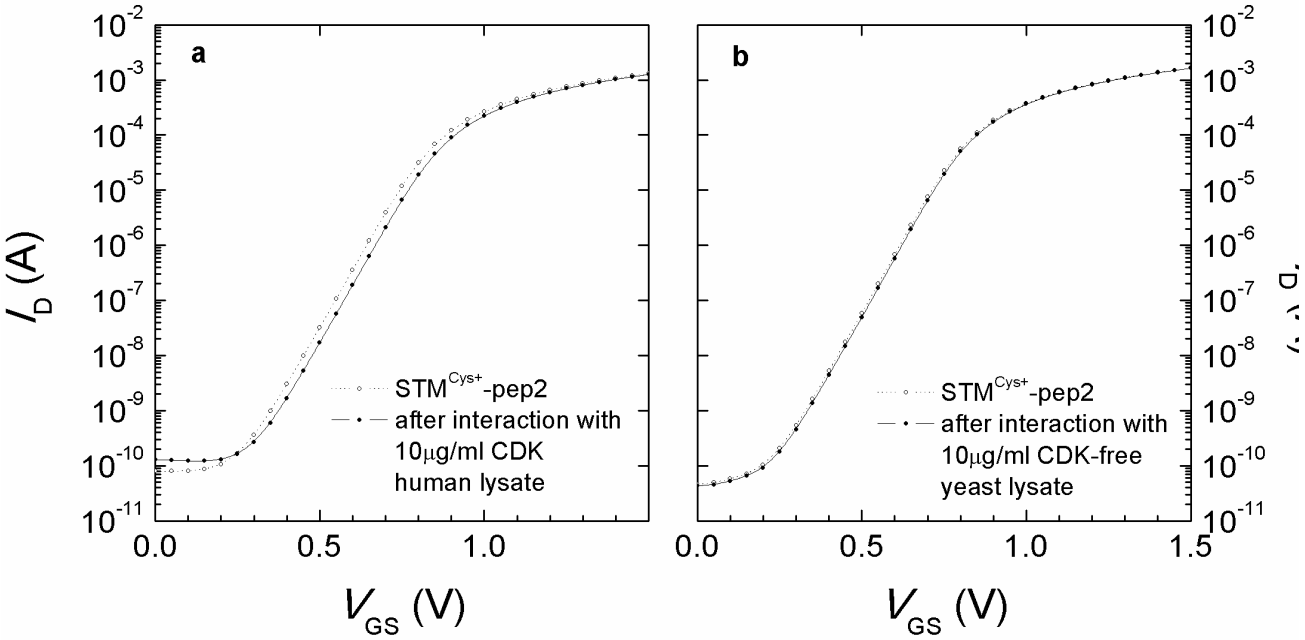

Figure 3. Transfer characteristics of two n-channel transistors with sizes W/L = 1630 µm/1.6 µm after immobilization of STM^{Cys+}–pep2 and after interaction with: (a) 10 µg/ml of human cell CDK2 lysate and (b) 10 µg/ml of CDK-free yeast lysate. V_{DS} was kept at 1 V. The error bars are smaller than the data points and were removed from the figure.

the specific interaction.[17] As a control, transistors functionalized with the peptide aptamer were exposed to a CDK-free yeast lysate, resulting in a small shift of +4.1 ± 4.4 mV (figure 3b) due to non-specific interaction with some of the proteins present in the lysate. Both lysates had a total protein concentration of 10 µg/ml.

The gold-thiol chemistry employed for the immobilization of STM^{Cys+}-pep2, ensures that the peptide aptamer orientation on the surface is controlled and regular with the peptidic inserts readily available for interaction with the target proteins. Bound target is therefore expected to form a defined layer within the electrochemical double-layer. This attribute of interfacial probe orientation is necessary to meaningfully consider the effect of the charge of the analyte onto the sensing gold pad.

As the concentration of CDK2 in the lysates is unknown, binding curves were acquired with solutions containing known concentrations of purified recombinant CDK2. The transfer characteristics of several transistors with STM^{Cys+}–pep2 immobilized on the extended gold electrodes were measured upon injection of CDK2 into the measurement buffer. Figure 4 shows the average gate voltage shifts observed on two transistors for CDK2 concentrations ranging from 21 fM (1.2 pg/ml) to 1.9 nM (110 ng/ml). Measurable signals were obtained even for the lowest concentrations. For protein concentrations of ~100 fM, shifts of the order of 1 mV (± 0.1 mV) are reproducibly measured.

The binding curve (Figure 4) is not expected to follow a traditional Scatchard-Rosenthal affinity model,[23] where the signal depends on the analyte concentration *c* and the dissociation constant K_d as $c/(K_d+c)$. This model assumes that the signal is directly proportional to the amount of bound target. In the present case, the measured potential variation has a non-linear dependence on the charge density: using the Gouy-Chapman-Stern model for the electrochemical double layer, the potential varies as the inverse hyperbolic sine of the charge density.[11] Furthermore, since the bound CDK will sit further away from the electrode than the Debye length, its charge will be partially screened by the electrolyte, which implies that the charge density of the bio-layer does not necessarily have a linear dependence on the amount of bound CDK. The binding curve seems to have a logistic-type behaviour characteristic of immunoassays, although a fit using a four-parameter logistic model[24] has not been possible presumably due to the low concentration range studied.

Even though the bound CDK2 is expected to extend over a large distance from the surface, large

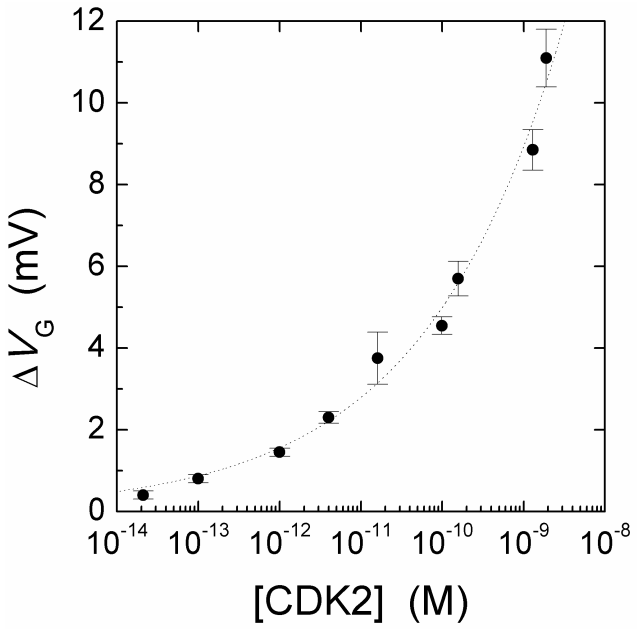

Figure 4. Gate voltage shifts observed at I_D = 1 µA for transistors functionalized with STM^{Cys+}–pep2 upon in-situ interaction with CDK2. The CDK2 concentrations were varied between 21 fM (1.2 pg/ml) and 1.9 nM (110 ng/ml). The data represent the average of the shifts obtained for 2 adjacent transistors with sizes W/L = 3860 µm/0.7 µm and W/L = 2670 µm/1.0 µm. The line is a guide to the eye.

signals are observed using the present MOSFET configuration. The nature of the signal is likely to be a combination of different effects. We have previously reported a negative shift of the OCP upon interaction and the concomitant increase of the charge transfer resistance, extracted from electrochemical impedance spectroscopy measurements with negative redox couple in solution.[17] This supports the explanation that the interaction produces a more negative potential barrier at the SAM/electrolyte interface, which is consistent with the observed shift of the transistor characteristics. That said, the situation here is quite different from the classical picture of a planar interface and uniform electrochemical double layer. Assessing the role of target position relative to the double layer, would require implementation of more sophisticated models, taking into account the discreteness of the charges and the fundamentally three-dimensional nature of the double layer.[25] Conformational changes of the biolayer upon interaction may also occur.[26]

The specificity of the interaction of different immobilized STM-based peptide aptamers to CDK proteins has been previously demonstrated by SPR,[16,21] QCM,[17] microcantilever,[20] electrochemical impedance spectroscopy,[17,19] dual polarization interferometry,[18] and direct OCP measurements.[17] The interaction can be turned off by changing or removing the peptide insert. For the MOSFETs here reported, control experiments carried out with immobilized scaffold adlayers without the recognition sequence (STM^{Cys+}) were associated with <5 mV shifts at high nanomolar CDK2 concentration. Analogous control experiments with the STM^{Cys+}–pep2 aptamer surface responded with shifts lower than 4 mV to high (micromolar) levels of BSA, indicating that further work is required to prevent non-specific interactions when large amounts of interfering compounds are present in the sample. Nevertheless, the present results suggest that stable MOSFETs with extended metal gates can be used for label-free electrical detection of proteins with an ultra-low detection limit.

CONCLUSIONS

Sub-picomolar label-free electrical detection of proteins has been achieved using MOSFETs in a novel approach. Gold electrodes externally connected to the gate contact pad of the MOSFETs act as extended gates for the transistors where biomolecular interactions take place. Using a peptide aptamer and a cell marker protein as a test system, protein concentrations of the order of 100 fM (or 5 pg/ml) have been detected. This the first time that such low protein concentrations have been detected using CMOS-based label-free electrical devices. The presented electrode configuration with the transistor buried under a passivation layer enables the use of low-cost CMOS processes for the fabrication of biologically-sensitive MOSFETs.

In the 1.5 ml measurement cell used, the low concentration detected corresponds to 9×10^7 protein molecules in the solution. Through appropriate design, the size of the gate electrode and the volume of the measurement cell can be reduced by two orders of magnitude or more, enabling, in theory, at these levels of sensitivity, detection of just a few thousand molecules. MOSFET-based sensors are intrinsically suited to miniaturization since the signal is independent of

the device size. Another advantage is that only a reference electrode is required, instead of the 3-electrode potentiostatic arrangement needed for current-based detection. A multiplexed array of MOSFET devices is presently being fabricated. The array will have the gold electrodes monolithically integrated on the chip.

ACKNOWLEDGMENT

The authors would like to thank Dr S.L. Thomas (Rutherford Appleton Laboratory) for providing the transistors. The authors acknowledge financial support from the Biotechnology and Biological Sciences Research Council UK under contract BB/D523094/1.

REFERENCES

(1) Schwaber, J.; Cohen, E.P. *Nature* **1973**, *244*, 444-447.

(2) Harlow, E.; Lane, D.P. *Antibodies: A Laboratory Manual*; Cold Spring Harbor Laboratory Press: New York, 1988.

(3) Kingsmore, S.F. *Nat. Rev. Drug Discov.* **2006**, *5*, 310–320.

(4) Cho, W.C.S. *Mol. Cancer* **2007**, *6*, 25.

(5) Stears, R.L.; Martinsky, T.; Schena, M. *Nat. Med.* **2003**, *9*, 140-145.

(6) Uttamchandani, M.; Wang, J.; Yao, S.Q. *Mol. BioSyst.* **2006**, *2*, 58-68.

(7) Kirby, R.; Cho, E.J.; Gehrke, B.; Bayer, T.; Park, Y.S.; Neikirk, D.P.; McDevitt, J.T.; Ellington, A.D. *Anal. Chem.* **2004**, *76*, 4066-4075.

(8) Herzog, G.; Arrigan, D.W.M. *Analyst* **2007**, *132*, 615-632.

(9) Vestergaard, M.; Kerman, K.; Tamiya, E.; *Sensors* **2007**, *7*, 3442-3458.

(10) Yu, X.; Xu, D.; Cheng, Q. *Proteomics* **2006**, *6*, 5493-5503.

(11) Estrela, P.; Migliorato, P. *J. Mater. Chem.* **2007**, *17*, 219-224.

(12) Haab, B.B.; Dunham, M.J.; O'Brown, P. *Genome Biol.* **2001**, *2*, 0004.

(13) Binz, H.K.; Amstutz, P.; Pluckthun, A. *Nat. Biotechnol.* **2005**, *23*, 1257-1268.

(14) Colas, P.; Cohen, B.; Jessen, T.; Grishina, L.; McCoy, J.; Brent, R. *Nature* **1996**, *380*, 548-550.

(15) Woodman, R.; Yeh, J.T.H.; Laurenson, S.; Ko Ferrigno, P. *J. Mol. Biol.* **2005**, *352*, 1118-1133.

(16) Davis, J.J.; Tkac, J.; Laurenson, S.; Ko Ferrigno, P. *Anal. Chem.* **2007**, *79*, 1089-1096.

(17) Estrela, P.; Paul, D.; Li, P.; Keighley, S.D.; Migliorato, P.; Laurenson, S.; Ko Ferrigno, P. *Electrochim. Acta* **2008**, *53*, 6489-6496.

(18) Johnson, S.; Evans, D.; Laurenson, S.; Paul, D.; Davies, A.G.; Ko Ferrigno, P.; Wälti, C. *Anal. Chem.* **2008**, *80*, 978-983.

(19) Evans, D.; Johnson, S.; Laurenson, S.; Davies, A.G.; Ko Ferrigno, P.; Wälti, C. *J. Biol.* **2008**, *7*, 3.

(20) Shu, W.M.; Laurenson, S.; Knowles, T.P.J.; Ko Ferrigno, P.; Seshia, A.A. *Biosens. Bioelectron.* **2008**, *24*, 233-237.

(21) Davis, J.J.; Tkac, J.; Humphreys, R.; Buxton, A.T.; Lee, T.A.; Ko Ferrigno, P. *Anal. Chem.* **2009**, *81*, 3314-3320.

(22) Madou, M.J.; Morrison, S.R. *Chemical Sensing with Solid State Devices*; Academic Press: San Diego, 1989.

(23) Pedersen, J.B.; Lindup, W.E. *Biochem. Pharmacol.* **1994**, *47*, 179-185.

(24) Dudley, R.A.; Edwards, P.; Ekins, R.P.; Finney, D.J.; McKenzie, I.G.M.; Raab, G.M.; Rodbard, D.; Rodgers, R.P.C. *Clin. Chem.* **1985**, *31*, 1264-1271.

(25) Keighley, S.D. PhD Thesis; University of Cambridge, 2008.

(26) Gupta, S.; Elias, M.; Wen, X.; Shapiro, J.; Brillson, L.; Lu, W.; Lee, S.C. *Biosens. Bioelectron.* **2008**, *24*, 505-511.